

Akansel Cosgun* and Henrik I Christensen

Context Aware Robot Navigation using Interactively Built Semantic Maps

Abstract: We discuss the process of building semantic maps, how to interactively label entities in it, and use them to enable new navigation behaviors for specific scenarios. We utilize planar surfaces such as walls and tables, and static objects such as door signs as features to our semantic mapping approach. Users can interactively annotate these features by having the robot follow him/her, entering the label through a mobile app and performing a pointing gesture toward the landmark of interest. These landmarks can later be used to generate context-aware motions. Our pointing gesture approach can reliably estimate the target object using human joint positions and detect ambiguous gestures with probabilistic modeling. Our person following method attempts to maximize future utility by searching future actions, assuming constant velocity model for the human. We describe a simple method to extract metric goals from a semantic map landmark and present a human aware path planner that considers the personal spaces of people to generate socially-aware paths. Finally, we demonstrate context-awareness for person following in two scenarios: interactive labeling and door passing. We believe as the sensing technology improves and maps with richer semantic information becomes commonplace, it would create new opportunities for intelligent navigation algorithms.

Keywords: mobile robot navigation, semantic mapping, human-robot interaction

***Corresponding Author: Akansel Cosgun:** Georgia Institute of Technology, E-mail: akansel.cosgun@gmail.com

Henrik I Christensen: University of California, San Diego, E-mail: hichristensen@ucsd.edu

1 Introduction

Millions of robots around the world are in operation today, however most of them operate in factories, physically separated from humans. With the recent improvements in hardware and software systems, it is now becoming clear that robots can provide much more value

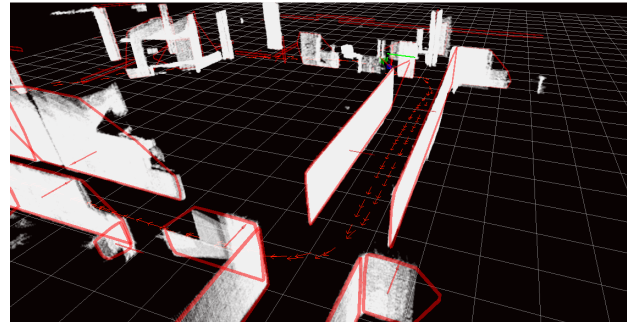


Fig. 1. An example of the type of map produced by our system. Planar features are visible by the red convex hulls, and red normal vectors. The small red arrows on the ground plane show the robot's trajectory. The point clouds used to extract these measurements are shown in white, and have been rendered in the map coordinate frame by making use of the optimized poses from which they were taken.

if they co-exist with humans in human environments including homes, hospitals and offices. The potential applications include, but not limited to autonomous delivery, elderly care, and household tasks such as cleaning. The feasibility and reliability of such applications will determine their business value. Therefore, any significant development in this field is a step toward realization of intelligent and social robots.

We are interested in developing mobile manipulators, which require more than just localization capabilities, but also need to understand the semantics of the space and spatial relationships with humans. Our mapping framework enables us to use a combination of features that leverage our prior knowledge of the environment to create maps that include task-relevant information. For example, our use of planar landmarks enable the robot to know the locations of tables, counters, and doors which are relevant to mobile manipulation tasks. Our framework additionally supports annotation of such landmarks, so that they can be referenced by name in interactions with users. Annotation of multiple rooms enable rooms to be labeled, and our use of door-sign landmarks enable room locations and numbers to be automatically added to the map during the

SLAM process. In our work on object discovery, modeling and mapping, we added support to our framework for object landmarks. Tabletop objects are discovered and modeled during the mapping process, and are used as landmarks. In summary, our SLAM framework enables us to create maps that include new types of task-relevant landmarks, including planes, lines, objects and additional constraints between these features that leverage our prior knowledge of semi-structured human environments to provide necessary information for service robotics tasks. In the context of mobile manipulators, this means that at the mapping process, we have a map that can not only localize the robot, but provide information to service robotic tasks about the locations of tables, rooms, doors and a set of object models discovered in the environment. These landmarks and objects can then be annotated by a user, so that they can be referenced by name in interactions. Knowledge of user-annotated landmarks can help robot navigation in two ways. First, the users and the robot can refer to the same landmarks by name and that would enable users to provide human-friendly navigation goals instead of goals in metric coordinates. Second, by knowing which room the robot currently is and whether there are relevant landmarks around such as tables and doors, the robot can display context-awareness. The navigation behaviors could be further improved by treating humans differently than obstacles.

The main contribution of this paper is a mapper that can create the types of maps required to enable context-aware navigation behaviors and facilitate communication of navigation goals between the humans and robots. To this end, we present a system capable of creating semantic maps and navigating intelligently among humans and user-labeled landmarks. We also describe the interaction model in which the user uses a combination of an app and natural pointing gestures to label landmarks.

The rest of this paper is organized as follows: A literature survey of related works is given in Section 2, followed by our semantic mapping approach in Section 3. Section 4 describes how users interactively label semantic elements, as well as components that enable labeling: person following and pointing gestures. In Section 5, we evaluate these sub-components. Section 6 discusses context-aware navigation behaviors and we conclude in Section 7.

2 Related Works

Research pertaining to semantic mapping and context-aware robot navigation has been ongoing for several years, and a large body of work exists that is related to this paper. In this section, we will provide a brief survey in the areas of semantic mapping (Section 2.1), human augmented mapping (Section 2.2), person tracking (Section 2.3) and context-aware mobile robot navigation (Section 2.4).

2.1 SLAM and Semantic Mapping

The Simultaneous Localization and Mapping (SLAM) problem was first proposed by Smith and Cheeseman [1], who used an Extended Kalman Filter (EKF) on landmark positions and the robot position. Many modern SLAM techniques, however, favor graph based representations over the EKF formulation. Instead of filtering and solving for only the current robot pose, these techniques typically maintain a graph of the entire robot trajectory in addition to the landmark positions, such as in [2]. Another area of interest is feature-based SLAM techniques, which use landmarks to solve the SLAM problem, such as the M-Space model [3].

Semantic mapping aims to build richer, more useful maps that include semantic information. Kuipers [4] proposed the Spatial Semantic Hierarchy (SSH), which is a qualitative and quantitative model of knowledge of large-scale space consisting of multiple interacting representations. This map also informs the robot of the control strategy that should be used to traverse between locations in the map. Martinez-Mozos [5] introduce a semantic understanding of the environment creating a conceptual representation referring to functional properties of typical indoor environments. Ekvall et. al [6] integrated an augmented SLAM map with information based on object recognition, providing a richer representation of the environment in a service robot scenario. Nuchter et.al investigated semantic labeling of points in 3D point cloud based maps in [7]. Semantic interpretation was given to the resulting maps by labeling points or extracted planes with labels such as floor, wall, ceiling, or door.

Semantic maps can also be used for other language based tasks, such as understanding commands like “get the mug on the table”. The robot can complete such tasks only if it knows the location and extent of the

table, can recognize mugs, and understands the meaning of “on”.

2.2 Human Augmented Mapping

Human Augmented Mapping was first introduced by Topp [8], where a human assists the robot in the map building process. This is motivated by the scenario of a human guiding a service robot on a tour of an indoor environment, and adding relevant semantic information to the map throughout the tour, for later reference. Users could ask the robot to follow them through out the environment and provide labels for locations, which could later be referenced in commands such as “go to label”. This means of providing labels seems quite intuitive, as users are co-located in the environment with the robot platform.

One of the key concepts in semantic mapping is that of “grounding”, or establishing “common ground” [9]. Of particular interest for mapping is grounding references, in order to ensure that the human and robot have common ground when referring to regions of a map, structures, or objects. Many spatial tasks may require various terms to be grounded in the map.

Dialog in human augmented mapping has been investigated in [10]. Clarification dialogs were studied in order to resolve ambiguities in the mapping process, for example, resolving whether or not a door is present in a particular location. This was applied to the Cosy Explorer system, described in [11], which includes a semantic mapping system that multi-layered maps, including a metric feature based map, a topological map, as well as detected objects.

2.3 Person Tracking

Laser-based methods remain one of the most commonly used approaches to person detection and tracking. The advantages of using laser scanners include high field of view and high accuracy. Legs in laser scans are typically distinguished using a multitude of geometric features [12]. Schulz [13] uses particle filters and statistical data association. Topp [14] demonstrates that leg tracking in cluttered environments is possible, but prone to false positives. Bellotto [15] combine leg detection and face tracking in a multi-modal tracking framework. Zanlungo [16] utilizes Social Forces Model to describe pedestrian motions, where parameters are trained with real pedestrian data.

Person tracking provides the robot with the position, and potentially orientation of the humans. However, richer information is typically needed for Human-Robot Interaction (HRI) applications. One of the common ways to refer places and objects to build common ground is to point at them. Pointing gestures are commonly used in HRI, such as for object references [17] and providing navigation goals [18]. After deciding if a pointing gesture occurred or not, typically the direction of pointing is also estimated. A commonly used method is to extend a ray from a body part to another and assume this ray is aimed toward the object of interest. The two of most commonly used methods are elbow-hand [19] and head-hand rays [17].

2.4 Context-Aware Navigation

Mobile robot navigation is traditionally seen as a shortest-path problem. While this leads to correct and collision-free paths, it may lead to sub-optimal robot behavior. The robot can exploit semantic information that is available to it and increase its effectiveness navigation capabilities. Context-aware navigation has found interest in two separate fronts: human-aware navigation and navigation using semantic information.

A common way to encode mobility constraints for navigating around humans is through costmaps. Sisbot [20] models the personal spaces as a ellipse-shaped Gaussian cost functions, and takes into account the safety and vision fields of humans. Kirby [21] presents a path planner that takes into account social conventions such as tending to one side of the hallways. One of the useful mobile robot applications that is widely studied is person following. A relevant body of work is pursuit evasion [22], in which the target is trying to evade the follower. In our applications, we assume that the target user is cooperating with the robot. Another body of work involves robot navigation in dense human traffic. Trautman [23] demonstrated a crowd navigation algorithm that performs comparably to human teleoperators. Kidokoro [24] simulates hypothetical situations using real data to anticipate how pedestrians’ walking comfort would be affected.

Some works considered using semantic information to improve robot navigation. Zender [25] considers context-awareness for person following, specifically handling of door and corridor passages. To handle door passages, the robot increases its following distance and that leads the robot to wait for a while. Person following in a corridor is handled with an approach similar to

Pacchierotti [26], and the robot’s speed is adjusted. Lu [27] show that using gaze cues makes robot-human hallway passing more efficient. Loper [28] presents a system that is capable of responding to verbal and non-verbal gestures and following a person.

3 Semantic Mapping

As service robots become increasingly capable and are able to perform a wider variety of tasks, we believe that new mapping systems could be developed to better support these tasks. Towards this end, we developed a simultaneous localization and mapping (SLAM) system that uses planar surfaces and objects as landmarks, and maps their locations and extent. We chose planar surfaces because they are prevalent in indoor environments, in the forms of walls, tables, and other surfaces. We also utilize door signs, and use this information to enhance robot navigation behavior.

Non-technical users will prefer human terms for objects and locations when assigning tasks to robots instead of whatever indices or coordinates the robot uses to represent them in its memory. Semantic mapping offers an advantage for robots to understand task assignments given to them by human users. We allow humans to label planar landmarks that is automatically acquired during the SLAM process, as described in Section 4. Users provide navigation goals in terms of these labeled landmarks. Our approach of finding goal points for a given planar landmark will be discussed in Section 6.1.1.

Planar landmarks provide semantic information about the space, as vertical planes correspond to walls, showing how space is partitioned, while horizontal planes correspond to tables and shelves, where objects of interest may occur. We describe in Section 3.2 how higher level objects, specifically door signs, can be used as landmarks in SLAM. We further explore in Section 6.2.2 how detection of door signs, therefore existence of doors, can be used for robot navigation.

3.1 Plane Landmarks

We believe that feature-based maps are suitable for containing task-relevant information for service robots. For example, a home service robot might need to know about the locations of structures such as the kitchen table and countertops, cupboards and shelves. Structures

such as walls could be used to better understand how space is structured and partitioned. We describe a SLAM system capable of creating maps of the locations and extents of planar surfaces in the environment using both 3D and 2D landmarks.

Our SLAM implementation makes use of the GTSAM library [2]. This library represents the graph SLAM problem with a factor graph which relates landmarks to robot poses through factors. GTSAM builds a factor graph of nonlinear measurements. Our approach involves using multiple types of landmark measurements as factors of nonlinear measurements. Planar surfaces can be detected in point cloud data generated by 3D sensors including tilting laser range finders, or RGB-D cameras such as the Microsoft Kinect or Asus Xtion. An example of a map produced by our system is shown in Figure 1.

A plane can be represented by the well known equation:

$$ax + by + cz + d = 0 \quad (1)$$

In this work, we make use of this representation, while additionally representing the plane’s extent by calculating the convex hull of the observed points. While only the plane normal and perpendicular distance are used for to correct the robot trajectory in SLAM, it is essential to keep track of the extent of planar patches, as many coplanar surfaces can exist in indoor environments, and we would like to represent these as distinct entities. We therefore represent planes as:

$$p = [n, hull] \quad (2)$$

where:

$$n = [a, b, c, d] \quad (3)$$

and *hull* is a point cloud consisting of the vertices of the plane’s convex hull. As planes are re-observed, their hulls are extended with the hull observed in the new measurements. That is, the measured hull is projected onto the newly optimized landmark’s plane using its normal, and a new convex hull is calculated for the sum of the vertices in the landmark hull and the measurement’s projected hull. In this way, the convex hull of a landmark can grow as additional portions of the plane are observed.

We use a Joint Compatibility Branch and Bound (JCBB) technique for data association [29]. JCBB works by evaluating the joint probability over the set of interpretation trees of the measurements seen by the robot at one pose. The output of the algorithm is the most likely interpretation tree for the set of measurements. We are

able to evaluate the probability of an interpretation tree quickly by marginalizing out the irrelevant portions of the graph of poses and features. The branch and bound recursion structure from the EKF formulation is used in our implementation.

Given a robot pose X_r , a transform from the map frame to the robot frame in the form of (R, \vec{t}) , a previously observed feature in the map frame (\vec{n}, d) and a measured plane (\vec{n}_m, \vec{d}_m) , the measurement function h is given by:

$$h = \begin{pmatrix} R^T * \vec{n} \\ \langle \vec{n}, \vec{t} \rangle + d \end{pmatrix} - \begin{pmatrix} \vec{n}_m \\ d_m \end{pmatrix} \quad (4)$$

The Jacobian with respect to the robot pose is then given by:

$$\frac{\partial h}{\partial X_r} = \begin{bmatrix} 0 & -n_a & n_b & [0] \\ n_a & 0 & -n_c & [0] \\ -n_b & n_c & 0 & [0] \\ 0 & 0 & 0 & \vec{n}^T \end{bmatrix} \quad (5)$$

The Jacobian with respect to the landmark is given by:

$$\frac{\partial h}{\partial n_{map}} = \begin{bmatrix} [R_r] & \vec{0} \\ X_r^T & 1 \end{bmatrix} \quad (6)$$

Using this measurement function and its associated Jacobians, we can utilize planar normals and perpendicular distances as landmarks in our SLAM system. During optimization, the landmark poses and robot trajectory are optimized.

3.2 Object Landmarks: Door Signs

The previous section introduced how we use planar landmarks for SLAM. In this section, we present a method for using a learned object classifier in a SLAM context to provide measurements suitable for mapping.

First, walls are extracted from straight lines in the laser scan. We use a RANSAC technique to extract lines from the laser data. Only lines which are longer than a certain threshold are passed to the mapper as measurements.

The door-sign-detector module makes use of a Support Vector Machine (SVM) classifier, trained on Histogram of Oriented Gradient (HOG) features. If an image region is classified as a sign by the SVM, then a query is made from this image region to the GoogleGoggles server. If GoogleGoggles is able to read any



Fig. 2. This sign is recognized and a measurement is made in the mapper. GoogleGoggles has read both the room number and the text, so this sign can be used for data association.

text on the sign, then it will be returned to us in a response packet. Detected signs with decoded text are then published as measurements that can be used by the mapper. The measurements consist of the pixel location in the image of the detected region’s centroid, the image patch corresponding to the detected region, and the text string returned from GoogleGoggles. An example detection of a door sign is shown in Figure 2.

Measurements generated by the door sign detector and laser line extractor modules are added as non-linear measurements to the factor graph. At the time of this study, we did not have a RGD-B sensor on the robot. Therefore, measurements were made on the 3D coordinates of the back-projected image location directly. Range is recovered by finding the laser beam from the head laser which projects most closely to the image coordinates of the sign. This technique approximates the true range. This factor also incorporates an additional variable which corresponds to the transformation between the robot base and the camera.

To implement this factor in GTSAM, we must specify an error function and the error function’s derivatives in terms of all of the variables which contribute to it. The error function is the difference in the 3D position of the predicted location of the sign from the measured value given by the recognition module.

4 Interactive Map Labeling

There are several methods to support the annotation of entities in a robot map. For example, while the robot is building its representation of the environment, it can recognize objects or landmarks such as doors, tables, rooms and automatically add these features to its map. Even though such a system would be useful, it may

wrongly label some objects. In that case, the correct label can be provided by a human with an interactive system. Custom labels would also allow custom annotations such as “Joe’s Room”.

We presented our method for building semantic maps in Section 3. We will assume that we have a metric and semantic map for the rest of this paper for simplicity. To enable a common ground between the humans and the robot, we developed an interactive procedure to annotate landmarks in the semantic map. In this procedure, the person guides the robot to the landmark of interest first and refers to the landmark of interest by pointing at it. The steps for labeling a landmark is shown in Figure 3. The robot follows the user around between labeling of landmarks. This allows the user to guide the robot to virtually any location in the environment. Our interactive map labeling approach was previously described in [30].

Various modalities could be used for the interaction model, such as speech or GUI-only. The reason why we combine the GUI with pointing gestures is that we think natural gestures would play an important role for human-robot interactions in the future.

For the rest of this section, we describe the sub-components necessary to realize interactive labeling, namely person following (Section 4.1), pointing gestures (Section 4.2) and object labeling (Section 4.3).

4.1 Person Following

The robot has to continuously estimate the position of the user in real-time for robust person following. We focus on tracking people who are either walking or standing, as these are the two most common human poses around a mobile robot. The reason for using multiple detectors for the person tracking system is to increase the robustness and provide 360° coverage around the robot. Below are the brief descriptions of the person detection methods:

1) Leg Detector: A front-facing laser scanner at ankle height (Hokuyo UTM 30-LX) is used. We trained a leg classifier using three geometric features: Width, Circularity and Inscribed Angle Variance [31]. We find a distance score for each candidate segment using the weighted sum of the distance to each feature and then threshold the score for detection.

2) Torso Detector: A back-facing Hokuyo laser scanner, placed at torso-level is used for this detector. We model the human torso as an ellipse and fit each segment in the laser an ellipse. The ellipse fitting approach

always returns a result, even for bad data. In addition to the geometric features we use for legs, we use two additional features for torso detection: The horizontal and vertical axes of the fitted ellipse. Similar to leg detection, we use a threshold test for the detection result.

The output of the detectors are input to a state estimation module. Using a state predictor for human movement has two advantages. First, the predicted trajectories are smoother than raw detections. Smooth tracking helps the robot maintain consistent trajectories for person following. Second, it provides a posterior estimate that can be used for data association when there is a lack of matching detections. This allows the tracker to handle temporary occlusions. We use a Linear Kalman Filter (KF) with constant velocity model to estimate the position and velocity of a person. We used a KF for tracking because it has acceptable tracking performance and is computationally cheap, which is important in real-time applications.

For person following, the robot uses the most probable location of the KF, which is the mean of the Gaussian distribution. We use Dynamic Window Approach (DWA) [32] at the core of our planner to sample velocity and acceleration-bounded trajectories, with the modification of using time as an additional dimension. DWA forward-simulates allowable velocities and chooses an action that optimizes a function that will create a goal-directed behavior while avoiding obstacles. Our approach projects the future locations of the target, creates a tree of trajectories, and scores each tree node according to a goal function, which is a function of the relative pose of the robot with respect to the human. Our planner takes the laser scan measurement, predicted positions of the person, and the number of time steps to plan as input and outputs a sequence of actions. A robot configuration at time t is expressed as $q^t = (x^t, y^t, \theta^t, v^t, \omega^t)^T$, where x^t and y^t denote positions, θ^t is the orientation, v^t and w^t are the linear and angular velocities at time t . The person configuration p^t is defined the same way. An action of the robot is defined as a velocity command for some duration: $a(t, \Delta t) = (v_a^t, \omega_a^t, \Delta t)$. We assume a unicycle kinematics model for trajectory sampling. Using this model, we generate a tree up to a fixed depth, starting from the current configuration of the robot. A tree node consists of a robot configuration as well as the information about the previous action and parent node. Every depth of the tree corresponds to a discretized time slice. Therefore, every action taken in the planning phase advances the time by a fixed amount. This enables the planner to consider future steps of the person and simulate what is

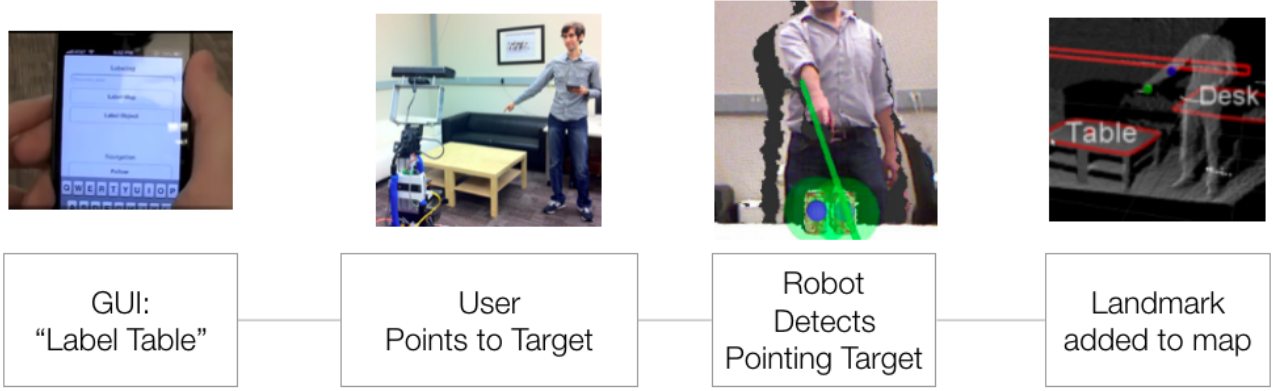


Fig. 3. Steps for interactively labeling a landmark in the semantic map. First, the user activates person following using the app. User stops nearby the target landmark, and enters the requested label using the app. Then the user performs a pointing gesture toward the target and waits for acknowledgement. Robot assesses the likelihood of nearby objects being the intended target, and asks for confirmation if ambiguity is detected. Finally, a string label is attached to the corresponding landmark in the semantic map.

likely to happen in the future. The planner uses depth-limited Breadth First Search (BFS) to search all the trajectories in the generated tree and determines the trajectory that will give the robot the maximum utility over a fixed time in the future. Given the robot and person configuration at some particular time, goal function $0 \leq g(q^t, p^t) \leq 1$ determines how desirable the situation is for the task. Goal function can be defined in any way and provides flexibility to the navigation behavior designer. We assume that it is desirable for the robot to follow from behind as it would give the robot a better chance to predict the human’s motions and implicitly mimic human’s path, which is known to be obstacle free. We report our results on this person following method in Section 5.1. In previous work, we applied this following method on an autonomous telepresence robot [33].

Another important capability to enable interactive labeling is to be able to refer to the same landmarks in the environment. Our design involves the person extending his/her arm and point at the landmark of interest. The method for detecting the pointing target is described next.

4.2 Pointing Gestures

In this section, we present an uncertainty model for estimating pointing gesture targets, based on previous work [34]. Estimating this uncertainty allows us to interpret whether a pointing gesture is ambiguous or not, when objects are too close to one another. We model the uncertainty of pointing gestures using a spherical coordinate system. We use this model to determine the cor-

rect pointing target, and detect when there is ambiguity. Two pointing methods, elbow-hand and head-hand rays, are evaluated using a 3rd party skeleton tracking algorithm, OpenNI NITE in Section 5.2.

We use a simple gesture detection algorithm as our focus is to estimate the gesture target given that a pointing gesture was performed. Using the skeleton data, pointing gestures are recognized if a human’s forearm makes more than a fixed angle with the vertical axis and elbow and hand joints stay almost stationary for a fixed duration. Gesture detection is activated only after the user requests a labeling action. This design is intended to reduce false positive detections.

We represent a pointing ray in two angles: a “horizontal” sense we denote as θ and a “vertical” sense we denote as ψ . We first attach a coordinate frame to the hand point, with its z-axis oriented in either Elbow-hand \vec{v}_{eh} or Head-Hand \vec{v}_{hh} directions. The hand was chosen as the origin for this coordinate system because both of head-hand and elbow-hand pointing methods include the user’s hand. The transformation between the sensor frame and the hand frame ${}^{sensor}T_{hand}$ is calculated by using an angle-axis rotation method. An illustration of the hand coordinate frame for Elbow-Hand method and corresponding angles are shown graphically in Figure 4.

Given this coordinate frame and a potential target point P, we first transform it to the hand frame by:

$${}^{hand}p_{target} = T_{hand} * p_{target} \quad (7)$$

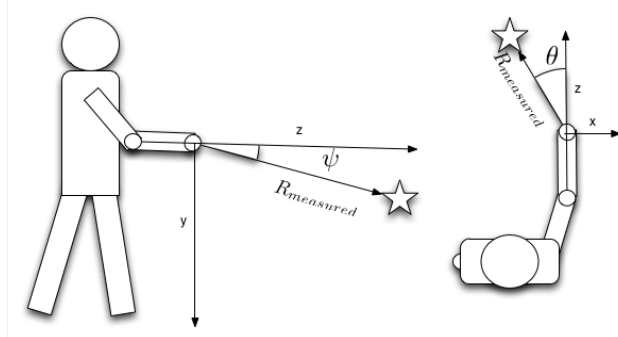


Fig. 4. Vertical (ψ) and horizontal (θ) angles in spherical coordinates are illustrated. A potential intended target is shown as a star. The z-axis of the hand coordinate frame is defined by either the Elbow-Hand (this example) or Head-Hand ray.

We calculate the horizontal and vertical angles for a target point as ${}^{hand}p_{target} = (x_{target}, y_{target}, z_{target})$ follows:

$$[\theta_{target} \ \psi_{target}] = [atan2(x_{target}, z_{target}) \ \atan2(y_{target}, z_{target})] \quad (8)$$

Where $atan2(y, x)$ is a function returns the value of the angle $\arctan(\frac{y}{x})$ with the correct sign.

We estimate the likelihood of objects being the target using statistical data from previous pointing gesture observations. We observed that head-hand and elbow-hand methods returned different angle errors depending on the target location. Our approach relies on finding error statistics of these approaches, and compensating the error when the target object is searched for. First, given a set of prior pointing observations, we calculate the mean and variance of the vertical and horizontal angle errors for each pointing method. This analysis will be presented in Section 5.2. Given an input gesture, we apply correction to the pointing direction and find the Mahalanobis distance to each object in the scene.

When a pointing gesture is recognized, and the angle pair $[\theta_{target} \ \psi_{target}]$ is found, and then a correction is applied by subtracting the mean terms from measured angles:

$$[\theta_{cor} \ \psi_{cor}] = [\theta_{target} - \mu_{\theta} \ \psi_{target} - \mu_{\psi}] \quad (9)$$

We also compute a covariance matrix for angle errors in this spherical coordinate system:

$$S_{type} = \begin{bmatrix} \sigma_{\theta} & 0 \\ 0 & \sigma_{\psi} \end{bmatrix} \quad (10)$$

We get the values for $\mu_{\theta}, \mu_{\psi}, \sigma_{\theta}, \sigma_{\psi}$ from Table 2 for the corresponding gesture type and closest target

location. We then compute the mahalanobis distance to the target by:

$$D_{mah}(target, method) = \sqrt{[\theta_{cor} \ \psi_{cor}]^T S_{method}^{-1} [\theta_{cor} \ \psi_{cor}]} \quad (11)$$

We use D_{mah} to estimate which target or object is intended. We consider two use cases: the objects are represented as a point or a point cloud. For point targets, we first filter out targets that have a Mahalanobis distance larger than a threshold $D_{mah} > D_{thresh}$. If none of the targets has a D_{mah} lower than the threshold, then we decide the user did not point to any targets. If there are multiple targets that has $D_{mah} \leq D_{thresh}$, then we determine ambiguity by employing a ratio test. The ratio of the least D_{mah} and the second-least D_{mah} among all targets is compared with a threshold to determine if there is ambiguity. If the ratio is higher than a threshold, then the robot can resort to additional action, such as initiating a dialogue to ask or confirm the intended object.

4.3 Labeling Object Models

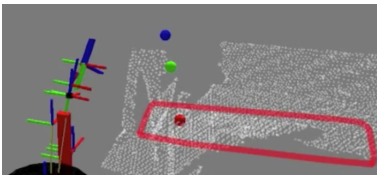
Our method supports labeling two types of landmarks: planar surfaces and objects. The UI shows two labeling buttons “Label Object” and “Label Planar Surface”, so that the robot knows what the user is intending to label. Section 4.2 demonstrated how point targets or point cloud targets can be referenced via pointing gestures. The referenced object is then annotated with the label entered by the user, and can then be recognized later as described in our previous work [35]. Figure 5 shows the steps the robot executes for this task. Service robotic tasks that use such a map can then reference the object by label, rather than generating a more complex referring expression (e.g. “the large object” or “the object on the left”).

5 Evaluation of Sub-Components

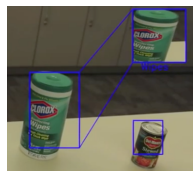
In this section, we evaluate two of the core sub-components that enables building interactive semantic maps. In Section 5.1 we analyze the person following behavior and in Section 5.2 we evaluate our pointing gesture target estimation method.



(a)



(b)



(c)

Fig. 5. a) A user pointing at an object. b) A detected pointing gesture (blue and green spheres), and referenced object (red sphere). c) Features are extracted from an image patch corresponding to the cluster, and annotated with the provided label.

5.1 Evaluation of Person Following

In this section, we report on an analysis of the person following sub-component. In our experiments, the robot followed 7 people for 3 laps and we logged the total distance robot followed the person and the average distance to the person. Users did not have prior experience with the robot and was asked to walk in a corridor while the robot is following them. A lap consisted of leaving the starting point, going to an intermediate point at the end of the corridor and coming back to the starting point from the same path. Table 1 shows the data pertaining this study. In total, the robot followed people for about 1.2km. The average distance between the person and the robot across all 7 runs was 1.16m (Table 1).

Subject #	Distance (m)	Avg. Dist to Person (m)
1	171.4	1.1
2	161.8	1.13
3	160.4	1.14
4	169.9	1.25
5	174.2	1.04
6	166.2	1.3
7	171.5	1.2

Table 1. Performance of the person follower on 7 subjects

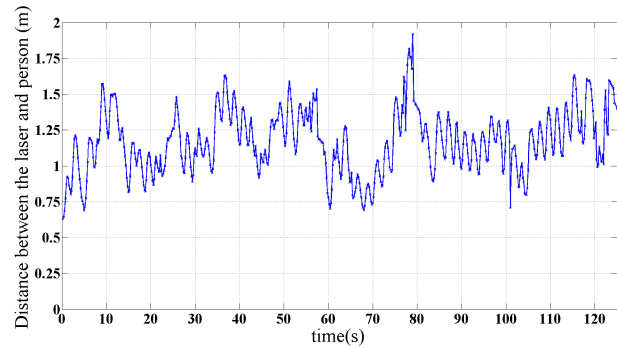


Fig. 6. Following distance as a function of time for one of the person following experiments.

Figure 6 plots the time versus following distance for a sample run that consists of 1 lap. At $t = 0$, the following is initiated and robot leaves the starting point. Around $t = 8s$, the robot and the person start making a right turn. The sudden drop in following distance at $t = 57.2$ signifies that the robot lost track of the person and the person tracker is reinitialized. At $t = 65.6s$, the intermediate point at the end of the corridor is reached so the person makes a 180° turn. The robot is close to the person (about $0.75m$) around this time because the robot is rotating around itself while the person is turning back. Between $t = 70$ and $t = 80s$, the person walks faster than the robot, so the following distance reaches to a maximum of $1.91m$. At $t = 79.8s$, the person is lost again. Around $t = 115s$, the robot and the person make a left turn. The lap ends at $t = 124s$. Note that the high frequency fluctuation of the following distance is a result of tracking only a single leg.

5.2 Evaluation of Pointing Gestures

To evaluate the accuracy of pointing gesture target detection, we first find the error statistics for pointing gestures, then apply it to a scenario for distinguishing two objects with varying separation.

We collected data from 6 users, with 7 targets, where people pointed at each target with their right arms (Figure 7). Our use case is on a mobile robot platform capable of positioning itself relative to the user. For this reason, we can assume that the user is always centered in the image, as the robot can easily rotate to face the user and can position itself at a desired distance from the user. The ground truth points, represented in the camera frame is found by first finding the pixel values of targets using a corner detector, extending a virtual ray from camera origin to a target and finding the



Fig. 7. Our study involved 6 users that pointed to 7 targets while being recorded using 30 frames per target.

intersection point to the supporting plane, which is extracted from the point cloud data. We computed the mean and standard deviations of the angular errors in the spherical coordinate system for each pointing gesture method and target.

The error statistics for Target 2 and across all targets are given in Table 2. The reason for reporting Target 2 only is that we use the error statistics of that target for the object separation study. From the data, we can tell that for the elbow-hand pointing method users typically point about 11° to the left of the intended target direction, and about 9° above the target direction. Similarly, the data from the head-hand pointing method reports that users typically point about 2° to the left of the intended pointing direction, but with a higher standard deviation than the elbow-hand method. On average, the vertical angle ψ was about 5° below the intended direction with a higher standard deviation than the elbow-hand method. The horizontal angle θ has a higher variation than the vertical angle ψ . Examining the errors for individual target locations shows that this error changes significantly with the target location. Therefore for a given target location, we first choose the closest target category in our data set, and use the corresponding mean and standard deviation values.

Next, we conducted an experiment to determine how our approach distinguished two potentially ambiguous pointing target objects. The setup consisted of a table between the robot and the person and two coke cans on the table (Figure 8) where the separation between objects was varied. The center positions of objects were calculated in real-time by a point cloud segmentation with supporting plane assumption. The separation between objects were varied with 1 cm increments from 2cm to 15cm and with 5cm increments between 15cm – 30cm. We could not conduct the experiment be-

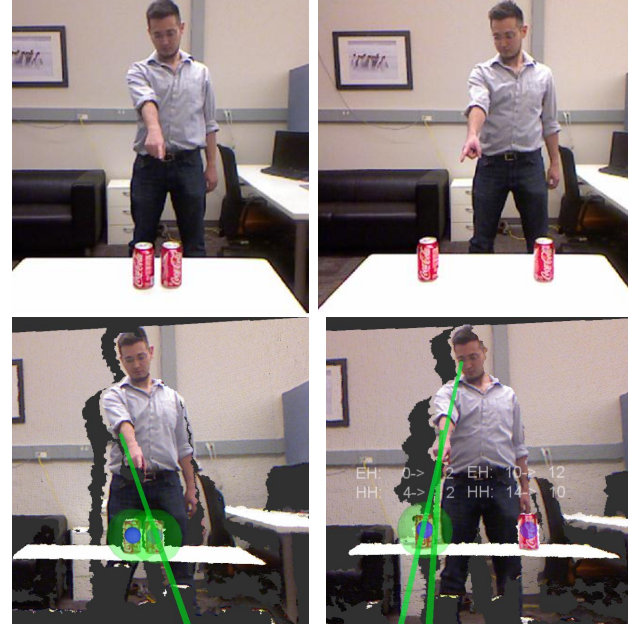


Fig. 8. Example scenarios from the object separation test is shown. Our experiments covered separations between 2cm (left images) and 30cm (right images). The object is comfortably distinguished for the 30cm case, whereas the intended target is ambiguous when the targets are 2cm apart. Second row shows the point cloud from the RGB-D camera’s view. Green lines show the Elbow-Hand and Head-Hand directions whereas green circles show the objects that are within the threshold $D_{mah} < 2$.

low 2cm separation because of the limitations of our perception system. The experiment was conducted with one user, who was not in the training dataset. For each separation, the user performed five pointing gestures to each object. The person pointed to one of the objects and the Mahalanobis distance D_{mah} to the intended object and the other object is calculated. Error statistics of Target 2 (Figure 7) was used for this experiment.

The results of the object separation experiment is given for Elbow-Hand (Figure 9(a)) and Head-Hand (Figure 9(b)) methods. The graphs plot object separation versus the Mahalanobis distance for the intended unintended objects, for corrected and uncorrected pointing gestures. First, the Mahalanobis distance D_{mah} for the intended object was always lower than the other object. The corrected D_{mah} for both Elbow-Hand and Head-Hand methods for the intended object was always below 2, therefore selecting the threshold $D_{thres} = 2$ is a reasonable choice. We notice that some distances for the unintended object at 2cm separation is also below $D_{mah} < 2$. Therefore, when the objects are 2 cm apart, then the pointing target becomes ambiguous for this setup. For separations of 3cm or more, D_{mah} of the unintended object is always over the threshold, there-

	Target 2				All Targets			
	θ		ψ		θ		ψ	
	μ	σ	μ	σ	μ	σ	μ	σ
Elbow-Hand	-3.8	6.6	11.3	10.9	-11.2	7.6	9.6	6.3
Head-Hand	10.2	6.7	-5.7	8.0	-2.4	9.6	-5.3	6.4

Table 2. μ and σ of angular errors (in degrees) are given for Target 2 and across all targets. Error statistics of Table 2 was used for the object separation evaluation. Reader is referred to [34] for the complete table.

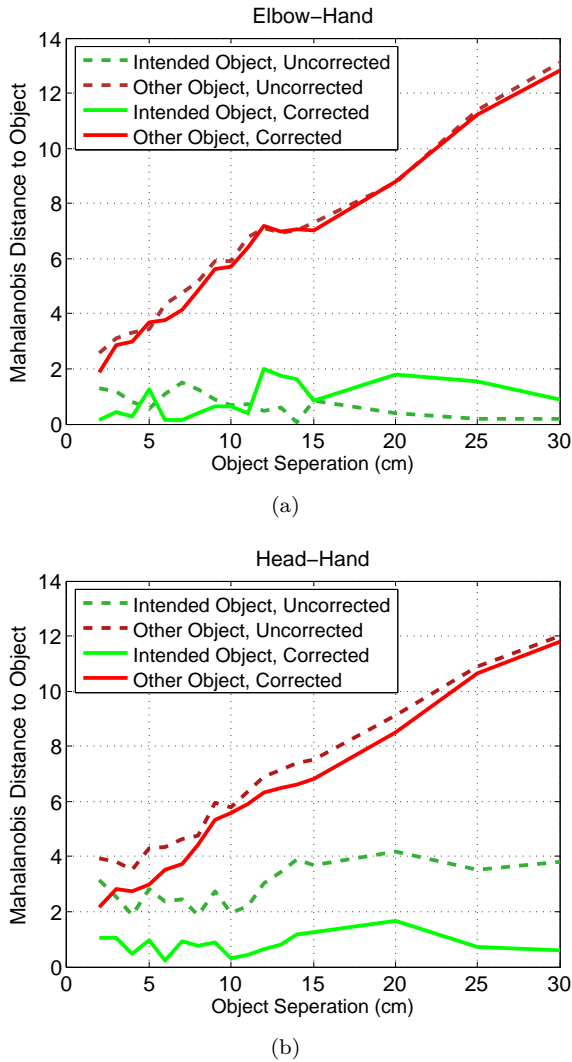


Fig. 9. Resulting Mahalanobis distances of pointing targets from the Object Separation Test is shown for a) Elbow-Hand and b) Head-Hand pointing methods. Intended object are shown in green and other object is in red. Solid lines show distances after correction is applied. Less Mahalanobis distance for intended object is better for reducing ambiguity.

fore there is no ambiguity. Second, correction significantly improved Head-Hand accuracy at all separations, slightly improved Elbow-Hand between 2-12cm but slightly worsened Elbow-Hand after 12cm. Third,

the Mahalanobis distance stayed generally constant for the intended object, which was expected. It linearly increased with separation distance for the other object. Fourth, patterns for both methods are fairly similar to each other, other than Head-Hand uncorrected distances being higher than Elbow-Hand.

6 Robot Navigation using Semantic Maps

Autonomous navigation is one of the most fundamental capabilities for a mobile robot. There are many approaches that achieve point-to-point autonomous navigation thanks to the advances in mapping, localization and motion planning research. Many of these algorithms are optimized to find the least-cost path, or the shortest path. However, often there are additional social factors to consider for navigation among humans.

First, it is not natural for humans to provide the goals in exact coordinates. Instead, the robot should be able to understand goals that are expressed natural language and grounded with shared references. In our approach, users provide annotated landmarks as goals to the robot using a mobile app. Our method of goal calculation from a user query is discussed in Section 6.1.1.

Second, robots should pay special attention to their motions when there are humans in the environment, or when there is a probability of encountering a human. For example, while it is acceptable for a robot to get very close to a wall, doing so to a human is socially unacceptable and unsafe. Similarly, sudden appearance of a robot can surprise humans and cause discomfort. There are many other social scenarios where the shortest path may not be optimal. Therefore context-aware path planning algorithms should treat humans and obstacles differently to enable intelligent robot behaviors. Our human-aware path planning method is described in Section 6.1.2.

Third, semantic maps could be exploited to enhance navigation behaviors. Robot navigation behaviors could be tailored to the task at hand. For example, when the robot is following a person during the map labeling task, the robot chooses its sub-goals to facilitate interaction. Similarly, semantic maps could be useful to negotiate passing in bottlenecks, such as door passages. We present our context-aware person following approach in Section 6.2, built on top of the person following method presented in Section 4.1.

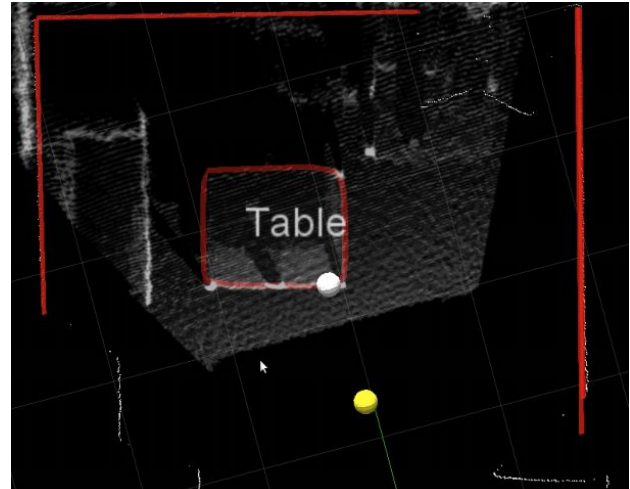
6.1 Navigating to Labeled Landmarks

6.1.1 Finding the Goal Point

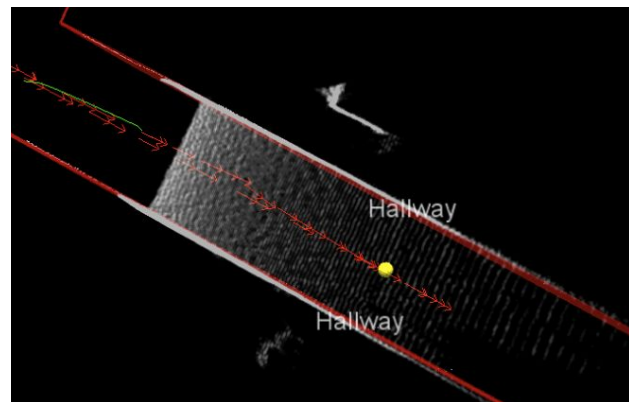
In our current application, the goals are either labeled landmarks or objects using a phone/tablet app. When a user enters a landmark as a navigation goal, the robot first finds a goal point in the metric map, then plans and executes a socially acceptable path toward this goal.

When a planar landmark is entered as the goal, the metric goal is chosen towards the closest edge of the plane. We first select the closest vertex on the landmark’s convex hull to the robot’s current position, and project it to the floor plane. We find the line between the closest vertex on the convex hull and the robot’s current pose. The goal position is selected to be on this line, a meter away from the vertex. With this design, robot would reach to close proximity of the desired planar surface and be oriented towards it. This method is suitable for horizontal planes such as tables, and vertical planes alike, such as doors. An example for finding a goal pose for a uniquely labeled planar landmark is shown in Figure 10(a).

When there are multiple planes associated with the same label, then we interpret this landmark as a region or space, such as a room or corridor. In this case, we project the points of all planes with this label to the ground plane, and compute the convex hull. The goal position is chosen as the centroid of the convex hull and goal orientation is unspecified, meaning the robot would not change its orientation upon reaching the goal position. An example goal position where the goal landmark label “hallway” represents two walls enclosing a hallway is shown in Figure 10(b).



(a)



(b)

Fig. 10. a) Top down point cloud view of a room. A planar landmark with label *Table* has previously been annotated by a user. The convex hull for the planar landmark is shown in red lines. When asked to navigate to *Table*, the robot calculates a goal position, which is shown as the yellow point. b) Top down point cloud view of a hallway. The user has previously annotated two planar landmarks with the same label, *Hallway*. When asked to navigate to *Hallway*, the robot chooses a goal position in the middle of the planar landmarks, shown as the yellow point.

6.1.2 Human-Aware Path Planning

After a goal position is calculated, a socially acceptable path is planned starting from the current position of the robot. Most approaches divide the robot path planning problem into two: global and local planning. Our approach adopts this template, and further divides global planning into two parts: static and dynamic planners. Static planner finds a path on the map of the environment by considering the safety, disturbance of humans and path length and but doesn’t consider the future movements of humans. Dynamic planner simulates the

reaction of humans and refines the static path. Dynamic planner takes the static path and refines it by considering the predicted temporary goals of humans, reaction to the robot's future movements. Our local planner is essentially a trajectory planner that computes the linear and angular velocities that would allow the robot to follow the dynamic path. The navigation system overview is shown in Figure 11. More information about this work can be found in [36].

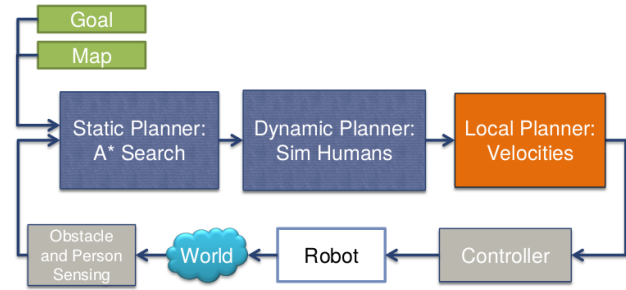


Fig. 11. System overview. When a map and goal is provided to the static planner, obstacles and humans are detected, then a path is planned using A* search. Dynamic planner refines the static plan by simulating human reactions to robot motion. Local planner receives the result, and computes the linear and angular velocities necessary to follow the path. The controller applies these velocities to the robot, which in turn acts in the world.

Static planner takes the start and goal positions and a 2D grid map as input and aims to find a set of waypoints that connects the start and goal cells. The output path has the minimum cost with regards to a linearly weighted cost function with 3 components: path length, safety and disturbance. We use A* search with Euclidean heuristics on a 8-connected grid map to find the minimum cost path. The path length cost is the total length of a path. The safety cost aims to model personal spaces of people. A gaussian cost function is attached to each person in the environment. The safety cost of a cell is the maximum safety cost value among all humans in the environment. Disturbance cost aims to represent the cases where the robot potentially disturbs the interaction of a group of humans. For example, if two people are facing each other and talking, then the robot should not cross between them. Disturbance cost is a non-zero cost if the robot's path crosses between two people who are in reasonable proximity to each other. We do not detect if there actually is conversation between the people, but estimate the disturbance cost using body poses of agents. This cost increases if body orientations of two people are facing each other and is

inversely proportional on the distance between a pair of humans.

The dynamic path refinement processes the static plan by simulating parts of the path where group of humans are closeby. We use Social Forces Model (SFM) [37] to simulate the motions of humans and the robot. Interaction between people are modeled as attractive and repulsive forces in SFM, similar to potential fields. The forces are recomputed iteratively and the resulting simulated paths replaces the corresponding path sections in the static plan. We use DWA as the local trajectory planner. The refinement steps allows considering future motions of humans due to the robot's future motions.

We demonstrate our approach with an example in simulation (Figure 12). The goal of the robot is to navigate to a goal position in an office environment where there are 4 people present in the environment. In this scenario, we show how the path changes significantly when only poses of humans are varied. There are 3 main ways the robot can navigate to its goal: left, center or right corridor.

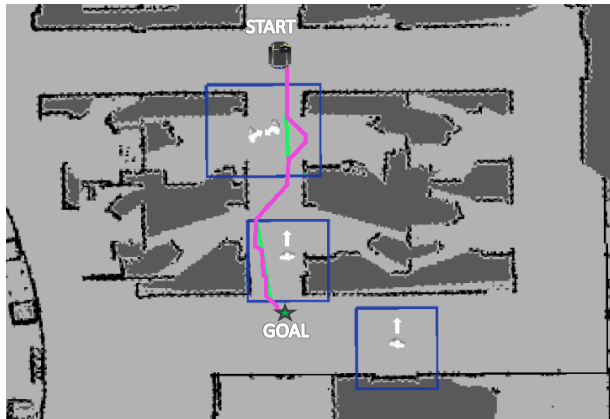
In the first configuration in Figure 12(a), two people are grouped together as they are looking at each other and likely conversing. The robot decides to take the center corridor, first slightly disturbing the speaking duo, then switches sides in the corridor and reaches its goal. In the figure, the dynamic path (pink line) is overlaid on the static path (green line).

In the second configuration in Figure 12(b), The third person at the center corridor joins the conversation. Now we have 2 group regions (rectangles) in the scene. Since passing through a group of 3 people would introduce a high disturbance cost in addition to the safety cost, the robot decides to take a longer route (left corridor). Since this path does not intersect any group regions, dynamic simulation was not conducted.

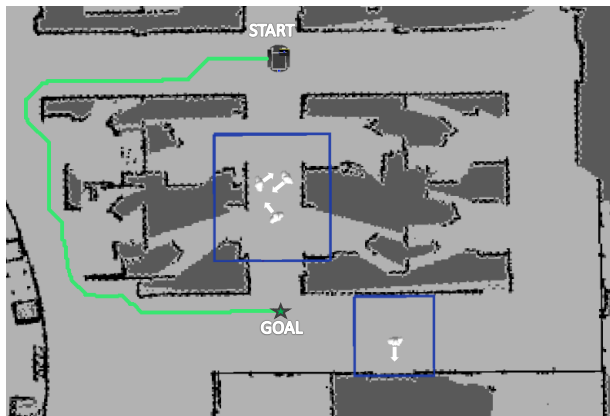
In the third configuration in Figure 12(c), the group of three hasn't moved, but the fourth person has changed its position. In this case, if the left corridor is taken again, an additional safety cost would be incurred. Therefore the robot decides to take the longest route (right corridor). Again, since the robot travels far from humans, dynamic simulation was not conducted.

6.2 Context-Aware Person Following

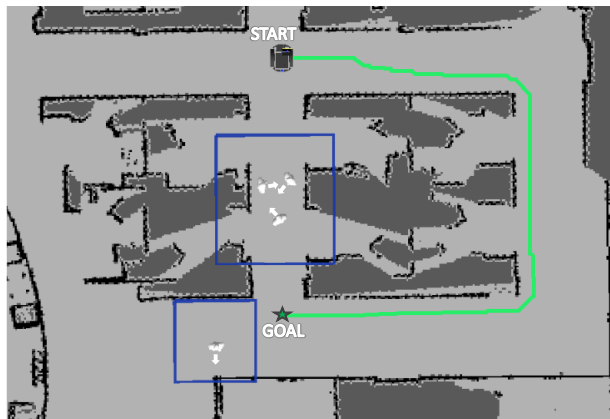
As briefly reviewed in Section 2.4, most person following methods in the literature have the same underlying principle: a target position is calculated given the human's



(a)



(b)



(c)

Fig. 12. Path planner's output differ given the poses and grouping of humans. a) The robot takes shortest route, traveling in the vicinity of a group of two and another individual. b) third individual joins the group. Robot takes a longer path that doesn't have humans on path. c) fourth person changes his position, leading the robot to take the longest route.

position and a control method finds actions iteratively to navigate toward the target positions. This results in

reactive robot behaviors where the robot follows the human blindly, irrespective of the task and context. Our person following method presented in Section 4.1 also falls under this category.

Although reactive methods are sufficient for some scenarios, it can easily lead to deadlock scenarios. For example, consider the case that the followed person goes through a door and stops just outside the doorway. In this case, the robot would occupy the doorway, blocking other people's passage, however does not know it caused an undesirable social situation. If the robot knows what the user intends to do, it can anticipate those actions and suitably adjust its behavior. Person following can be used in different contexts, such as for carrying luggage in airports or groceries in a supermarket. We showed in previous sections that semantic information could be used to communicate goals between the robot and the user. The stored semantic information can also be used to facilitate robot navigation.

We model the task scenario during person following as a state machine, where transitions are triggered via events. A general scenario during person following is implemented as a sequence of four phases:

1. Signal: Robot detects an event using perceptual cues
2. Approach: Robot moves to a position better suited to the task
3. Execution: Robot and/or Human execute the task
4. Release: Robot detects the end of event and continues with the basic following behavior

We focus on two specific scenarios of context-aware person following, using the 4-phase model: following for labeling in Section 6.2.1 and passing doors in Section 6.2.2. For both of the scenarios, we demonstrate the capability with a user who is knowledgeable of the robot's capabilities.

6.2.1 Following for Interactive Labeling

We first examine person following scenario for interactive labeling of semantic landmarks, as described in Section 4. For this scenario the robot follows the user as he/she moves between the landmarks or objects of interests. Sometimes when a user wants to label an object, undesirable social situations can occur because the robot does not have the task context. In this example, the context is defined as the understanding of being a part of a collaborative task: interactive labeling. When a user stops in front of a landmark or object to label it, if the robot stays behind, it can not perceive the point-

ing gesture and the landmark at the same time. This situation is illustrated in Figure 13.

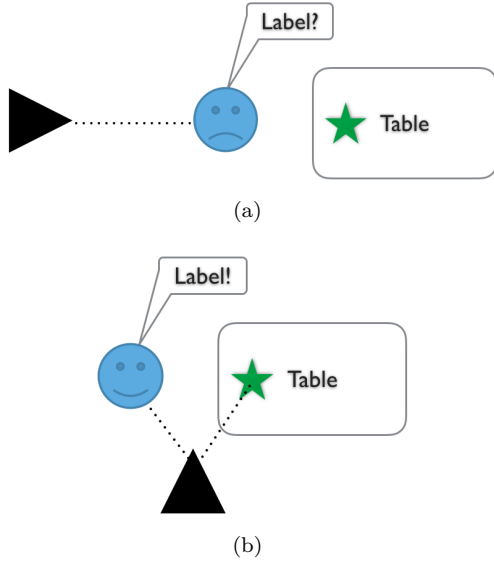


Fig. 13. a) A common problem encountered during person following for interactive labeling. The user wants to label an object on the table, however the robot does not know the user's intention and stays behind at a fixed distance to the user. b) Our solution is for the robot to navigate to a location that gives the robot a better chance to observe the user and the object simultaneously.

The robot can behave more intelligently if the robot can predict ahead of time when the user is going to label a landmark. When the robot detects that the user intends to label a landmark or object, our approach is to position the robot base so it has a better chance to perceive both the pointing gesture and the object/landmark of interest.

We follow the 4-phase behavior design for person following for interactive labeling. The Signaling phase is triggered whenever the user is close to a unlabeled landmark in the semantic map. The user must have close to zero speed to enable signaling for this behavior, because the user may walk past the landmark. After the robot detects the signal, we sample positions around the group to locate a "suitable" goal pose for the robot. A pose that is collision free but that gives the robot highest chance of interaction is favored. A suitable goal position should be at equal distance to the landmark and the user, and goal orientation should be selected so the robot faces in between the landmark and the user. Moreover, the goal point should not be very close to an obstacle. We linearly sample points around the "group" formed by the user and the landmark's centroid. The

points are sampled from the p -space of this group, which is a circle that includes the landmark and user center positions. This is influenced by Kendon's work [38] on how people form groups in interactive settings. Every sampled position p has a score of:

$$Score(p) = 1.0 - Cost_{vis}(p) - Cost_{obs}(p)$$

Where we define the costs as:

$$Cost_{vis}(p) = dist(user, LM) / (dist(p, LM) - dist(p, user))$$

$$Cost_{obs}(p) = max(local_cost(p), global_cost(p)) \quad (12)$$

The local and global costs are fetched from the normalized local costmap, which is formed by the laser scanner readings. The sample with the highest non-negative score is chosen as the goal position. The orientation of the robot is chosen as looking toward the center of all the people in the group.

When the robot completes its move to the goal position, the user labels the landmark or objects via pointing gestures. After the task is completed, the robot waits until the user to leaves the vicinity of the landmark. When that happens, the robot continues following the user. If, during any of the phases, the person tracking fails, it informs the user so following can be restarted. The phases and conditions for this behavior are summarized in Table 3. Images from a demonstration for this behavior is shown in Figure 14.

6.2.2 Door Passing

The second behavior we inspect during person following is door passing. In our experience, the a reactive person following behavior can cause problems while passing doors. For example, if the user intends to close an open door or open a closed door, the robot might end up blocking the movement of the door. Moreover, a deadlock situation occurs when the user wants to go through a door with spring-loaded hinges. In that case, the user would need to hold to door to keep it open, and because the distance between the robot and the user is less than the following threshold, the robot would stay still and won't pass the door.

The robot can assume that the user might be intending to open, close or pass through a door when the user is approaching the door. In our approach, the robot continuously monitors user's proximity to the doors using the semantic map, if the door signs were detected and added to the semantic map beforehand, as explained in Section 3.2.

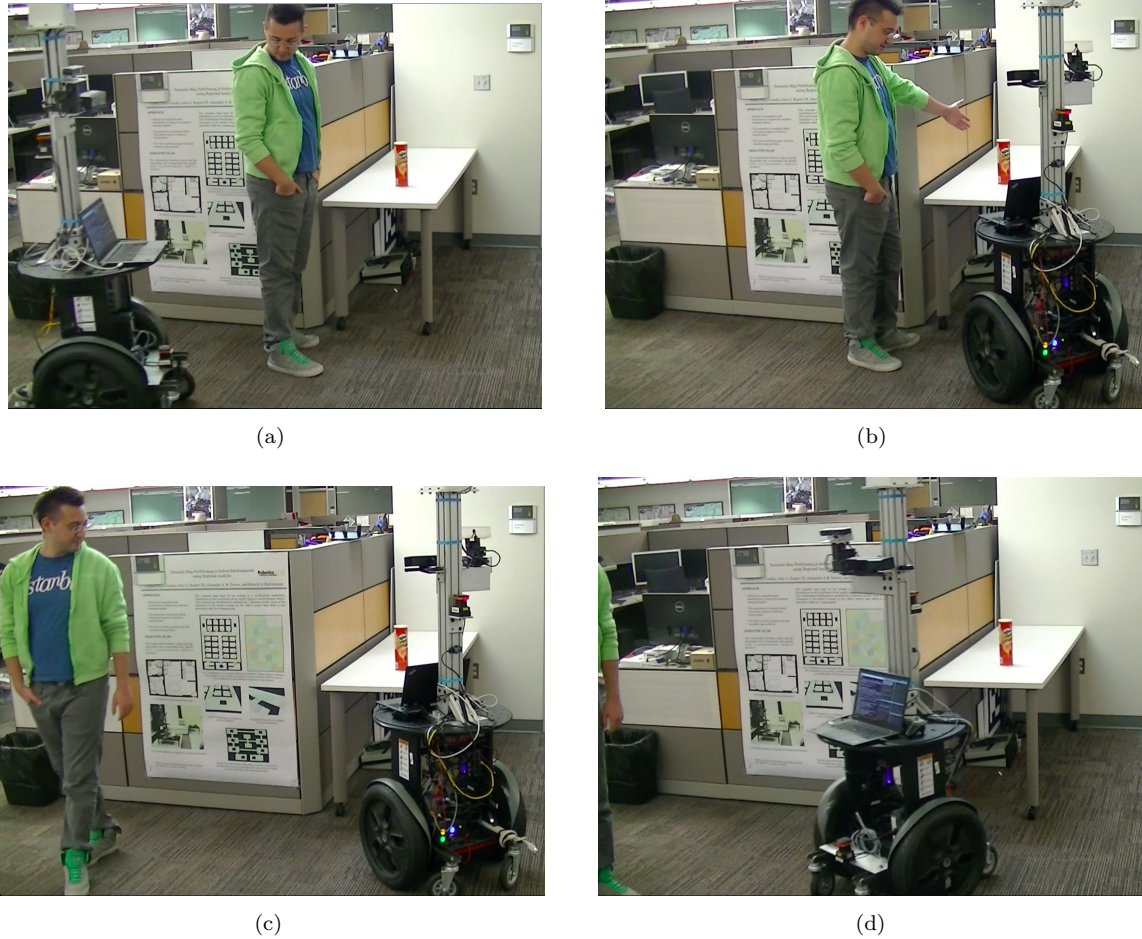


Fig. 14. Demonstration of context-awareness for interactive labeling. The robot is following the user throughout the environment and keeping a fixed distance of $1.2m$ to the user. a) Signal phase: The user has stopped and is in the cloxe proximity to the convex hull of the table. b) Approach phase: The robot calculates and navigates to a goal position, so it can perceive the pointing gesture and target. Execution phase: The user points out to the object on the table. c) Release phase: user moves away from the table d) Basic following behavior continues.

Signal	$dist(user, convexhull(landmark)) < threshold$ $speed(user) \sim 0$ person roughly facing landmark
Approach	Optimal Goal: Close to both the landmark and person, facing in between
Execution	User points and labels landmark
Release	$dist(user, convexhull(landmark)) > threshold$

Table 3. Conditions to trigger phases when the user is involved with the Landmark Labeling Event during following.

The phases and conditions for door passing situation are summarized in Table 4. The robot takes action when the user is nearby a door and performs a pointing gesture towards it, to signal that the robot should pass from the door (Signal Phase). If the action is not signaled, the robot continues with basic following during

the door passage. After the detection of a pointing gesture, a goal position is calculated (Approach Phase). The goal positions are sampled on the other side of the door, that is guaranteed not to block the opening/closing of the door. A collision-free position with the least obstacle cost sample is chosen as the goal point.

Signal	$dist(user, convexhull(door)) < threshold$ $speed(user) \sim 0$ User performs pointing gesture towards the passage
Approach	Optimal Goal: A position on the other side of the door that doesn't block the doorway
Execution	Robot and user meet at the same side of the door
Release	$dist(user, convexhull(door)) > threshold$

Table 4. Conditions to trigger phases when the user is passing through a door during following.

Note that while the robot is moving, it does not aim to keep fixed distance to the user anymore. After the robot reaches the goal, it waits for the person to pass the door (Execution Phase). After the user moved away from the door, the standard following behavior takes over. Images from the demonstration of context-aware person following for door passing is shown in Figure 15.

7 Conclusion

In this paper, we discussed the process of building semantic maps, how to interactively label entities in it, and use them to enable new navigation behaviors for specific scenarios. We utilize planar surfaces such as walls and tables, and static objects such as door signs as features to our semantic SLAM approach. Users can interactively annotate these features by having the robot follow him/her, entering the label through a mobile app and performing a pointing gesture toward the landmark of interest. These landmarks can later be used to generate context-aware motions.

Our pointing gesture approach can reliably estimate the target object using human joint positions and detect ambiguous gestures with probabilistic modeling. Our person following algorithm attempts to maximize future utility by searching future actions, assuming constant velocity model for the human. We showed that our person following method can keep a near-constant distance to the human. We described a simple method to extract metric goals from a semantic map landmark and presented a human-aware path planner that considers the personal spaces of people to generate socially-aware paths. Finally, we demonstrated context-awareness for person following in two scenarios: interactive labeling and door passing. For interactive labeling, the robot utilizes the task knowledge and moves to a favorable position to facilitate interaction if an unlabeled landmark is detected near the person. For door passing, the

robot utilizes the existence of a door passage, by querying detected door signs in the semantic map, to enter a door passage behavior.

Semantic maps would facilitate communication of goals from a HRI perspective and enable navigation behaviors that are not feasible with metric maps. We showed proof of concept for enabling context-aware navigation behaviors using semantics and believe that there is much to explore in this research area. We think as the sensing technology improves and maps with richer semantic information becomes common, it would make intelligent navigation algorithms possible.

One limitation of our work is that there is only implicit interaction between the robot and human in our interaction design. The robot signaled its intention only through motion and did not explicitly communicate with people. As future work, dialogue and gaze could be utilized to complement the motions of the robot.

We think implementation and qualitative validation of robot behavior is a critical first step for path planning algorithms among humans. In this paper, we showed that our approach produced sound solutions in a number of example scenarios. As future work, we think effectiveness of context-aware navigation could be evaluated with usability studies with users who are not familiar with the robot. Moreover, scenarios could be performed under different conditions to test the generality and validate the robustness of the system.

References

- [1] R. C. Smith and P. Cheeseman, "On the representation and estimation of spatial uncertainty," *The international journal of Robotics Research*, vol. 5, no. 4, pp. 56–68, 1986.
- [2] F. Dellaert and M. Kaess, "Square root sam: Simultaneous localization and mapping via square root information smoothing," *The International Journal of Robotics Research*, vol. 25, no. 12, pp. 1181–1203, 2006.



Fig. 15. Demonstration of context-awareness for door passing during person following. This is a swing door with spring loaded hinges, so it would close if not kept open actively. a) The robot is following the user by keeping a fixed distance to the user. b) Signal phase: The user has stopped, is in close proximity to the door and performed a pointing gesture toward the other room. c) Approach Phase: The robot passes the door while the user is holding the door d) Release Phase: User has more than a threshold distance to the door, and robot continues with the basic following.

- [3] J. Folkesson, P. Jensfelt, and H. I. Christensen, "The m-space feature representation for slam," *Robotics, IEEE Transactions on*, vol. 23, no. 5, pp. 1024–1035, 2007.
- [4] B. Kuipers, "The spatial semantic hierarchy," *Artificial intelligence*, vol. 119, no. 1, pp. 191–233, 2000.
- [5] O. M. Mozos, C. Stachniss, and W. Burgard, "Supervised learning of places from range data using adaboost," in *Robotics and Automation, 2005. ICRA 2005. Proceedings of the 2005 IEEE International Conference on*. IEEE, 2005, pp. 1730–1735.
- [6] S. Ekvall, D. Kragic, and P. Jensfelt, "Object detection and mapping for service robot tasks," *Robotica*, vol. 25, no. 02, pp. 175–187, 2007.
- [7] A. Nüchter and J. Hertzberg, "Towards semantic maps for mobile robots," *Robotics and Autonomous Systems*, vol. 56, no. 11, pp. 915–926, 2008.
- [8] E. A. Topp and H. I. Christensen, "Topological modelling for human augmented mapping," in *Intelligent Robots and Systems, 2006 IEEE/RSJ International Conference on*. IEEE, 2006, pp. 2257–2263.
- [9] H. H. Clark and S. E. Brennan, "Grounding in communication," *Perspectives on socially shared cognition*, vol. 13, no. 1991, pp. 127–149, 1991.
- [10] G.-J. M. Kruijff, H. Zender, P. Jensfelt, and H. I. Christensen, "Clarification dialogues in human-augmented mapping," in *Proceedings of the 1st ACM SIGCHI/SIGART conference on Human-robot interaction*. ACM, 2006, pp. 282–289.
- [11] H. Zender, P. Jensfelt, Ó. M. Mozos, G.-J. M. Kruijff, and W. Burgard, "An integrated robotic system for spatial understanding and situated interaction in indoor environments," in *AAAI*, vol. 7, 2007, pp. 1584–1589.
- [12] K. O. Arras, Ó. M. Mozos, and W. Burgard, "Using boosted features for the detection of people in 2d range data," in *Robotics and Automation, 2007 IEEE International Conference on*. IEEE, 2007, pp. 3402–3407.
- [13] D. Schulz, W. Burgard, D. Fox, and A. B. Cremers, "Tracking multiple moving targets with a mobile robot using parti-

- cle filters and statistical data association," in *Robotics and Automation, 2001. Proceedings 2001 ICRA. IEEE International Conference on*, vol. 2. IEEE, 2001, pp. 1665–1670.
- [14] E. A. Topp and H. I. Christensen, "Tracking for following and passing persons." in *IROS*, 2005, pp. 2321–2327.
- [15] N. Bellotto and H. Hu, "Multisensor-based human detection and tracking for mobile service robots," *Systems, Man, and Cybernetics, Part B: Cybernetics, IEEE Transactions on*, vol. 39, no. 1, pp. 167–181, 2009.
- [16] F. Zanlungo, T. Ikeda, and T. Kanda, "Social force model with explicit collision prediction," *EPL (Europhysics Letters)*, vol. 93, no. 6, p. 68005, 2011.
- [17] J. Schmidt, N. Hofemann, A. Haasch, J. Fritsch, and G. Sagerer, "Interacting with a mobile robot: Evaluating gestural object references," in *Intelligent Robots and Systems, 2008. IROS 2008. IEEE/RSJ International Conference on*. IEEE, 2008, pp. 3804–3809.
- [18] M. Van den Bergh, D. Carton, R. De Nijs, N. Mitsou, C. Landsiedel, K. Kuehnlitz, D. Wollherr, L. Van Gool, and M. Buss, "Real-time 3d hand gesture interaction with a robot for understanding directions from humans," in *RO-MAN, 2011 IEEE*. IEEE, 2011, pp. 357–362.
- [19] A. G. Brooks and C. Breazeal, "Working with robots and objects: Revisiting deictic reference for achieving spatial common ground," in *Proceedings of the 1st ACM SIGCHI/SIGART conference on Human-robot interaction*. ACM, 2006, pp. 297–304.
- [20] E. A. Sisbot, L. F. Marin-Urias, R. Alami, and T. Simeon, "A human aware mobile robot motion planner," *Robotics, IEEE Transactions on*, vol. 23, no. 5, pp. 874–883, 2007.
- [21] R. Kirby, R. Simmons, and J. Forlizzi, "Companion: A constraint-optimizing method for person-acceptable navigation," in *Robot and Human Interactive Communication, 2009. RO-MAN 2009. The 18th IEEE International Symposium on*. IEEE, 2009, pp. 607–612.
- [22] T. H. Chung, G. A. Hollinger, and V. Isler, "Search and pursuit-evasion in mobile robotics," *Autonomous robots*, vol. 31, no. 4, pp. 299–316, 2011.
- [23] P. Trautman, J. Ma, R. M. Murray, and A. Krause, "Robot navigation in dense human crowds: Statistical models and experimental studies of human–robot cooperation," *The International Journal of Robotics Research*, vol. 34, no. 3, pp. 335–356, 2015.
- [24] H. Kidokoro, T. Kanda, D. Brščić, and M. Shiomi, "Simulation-based behavior planning to prevent congestion of pedestrians around a robot," *IEEE Transactions on Robotics*, vol. 31, no. 6, pp. 1419–1431, 2015.
- [25] H. Zender, P. Jensfelt, and G.-J. M. Kruijff, "Human-and situation-aware people following," in *Robot and Human interactive Communication, 2007. RO-MAN 2007. The 16th IEEE International Symposium on*. IEEE, 2007, pp. 1131–1136.
- [26] E. Pacchierotti, H. I. Christensen, and P. Jensfelt, "Human-robot embodied interaction in hallway settings: a pilot user study," in *Robot and Human Interactive Communication, 2005. ROMAN 2005. IEEE International Workshop on*. IEEE, 2005, pp. 164–171.
- [27] D. V. Lu and W. D. Smart, "Towards more efficient navigation for robots and humans," in *Intelligent Robots and Systems (IROS), 2013 IEEE/RSJ International Conference On*. IEEE, 2013, pp. 1707–1713.
- [28] M. M. Loper, N. P. Koenig, S. H. Chernova, C. V. Jones, and O. C. Jenkins, "Mobile human-robot teaming with environmental tolerance," in *Proceedings of the 4th ACM/IEEE international conference on Human robot interaction*. ACM, 2009, pp. 157–164.
- [29] J. Neira and J. D. Tardós, "Data association in stochastic mapping using the joint compatibility test," *Robotics and Automation, IEEE Transactions on*, vol. 17, no. 6, pp. 890–897, 2001.
- [30] A. J. Trevor, A. Cosgun, J. Kumar, and H. I. Christensen, "Interactive map labeling for service robots," in *IROS Workshop on Active Semantic Perception*, 2012.
- [31] J. Xavier, M. Pacheco, D. Castro, A. Ruano, and U. Nunes, "Fast line, arc/circle and leg detection from laser scan data in a player driver," in *Robotics and Automation, 2005. ICRA 2005. Proceedings of the 2005 IEEE International Conference on*. IEEE, 2005, pp. 3930–3935.
- [32] D. Fox, W. Burgard, and S. Thrun, "The dynamic window approach to collision avoidance," *IEEE Robotics & Automation Magazine*, vol. 4, no. 1, pp. 23–33, 1997.
- [33] A. Cosgun, D. A. Florencio, and H. I. Christensen, "Autonomous person following for telepresence robots," in *Robotics and Automation (ICRA), 2013 IEEE International Conference on*. IEEE, 2013, pp. 4335–4342.
- [34] A. Cosgun, A. J. Trevor, and H. I. Christensen, "Did you mean this object?: Detecting ambiguity in pointing gesture targets," in *10th ACM/IEEE international conference on Human-Robot Interaction (HRI) workshop on Towards a Framework for Joint Action*. IEEE Press, 2015.
- [35] A. J. Trevor, J. G. Rogers III, A. Cosgun, and H. I. Christensen, "Interactive object modeling & labeling for service robots," in *Proceedings of the 8th ACM/IEEE international conference on Human-robot interaction*. IEEE Press, 2013, pp. 421–422.
- [36] A. Cosgun, E. A. Sisbot, and H. I. Christensen, "Anticipatory robot path planning in human environments," in *Robot and Human Interactive Communication (RO-MAN), 2016 25th IEEE International Symposium on*. IEEE, 2016, pp. 562–569.
- [37] D. Helbing and P. Molnar, "Social force model for pedestrian dynamics," *Physical review E*, vol. 51, no. 5, p. 4282, 1995.
- [38] A. Kendon, *Conducting interaction: Patterns of behavior in focused encounters*. CUP Archive, 1990, vol. 7.